Enhancement of intramolecular electron scattering due to molecule-electrode coupling in molecular junction systems

Hisashi Kondo
Institute of Industrial Science, University of Tokyo, 4-6-1 Komaba, Meguro-ku, Tokyo 153-8505, Japan and Computational Materials Science Center, National Institute for Materials Science (NIMS), 1-2-1 Sengen, Tsukuba, Ibaraki 305-0047, Japan

Jun Nara
Computational Materials Science Center, National Institute for Materials Science (NIMS), 1-2-1 Sengen, Tsukuba, Ibaraki 305-0047, Japan

Takahisa Ohno
Computational Materials Science Center, National Institute for Materials Science (NIMS), 1-2-1 Sengen, Tsukuba, Ibaraki 305-0047, Japan and Institute of Industrial Science, University of Tokyo, 4-6-1 Komaba, Meguro-ku, Tokyo 153-8505, Japan

(Received 6 August 2009; revised manuscript received 22 December 2009; published 12 February 2010)

We theoretically reveal that molecule-electrode coupling plays a crucial role in electron transport of molecular junction systems. It is found that as the coupling becomes stronger, transmission peaks are lowered despite the increasing of the wave function hybridization between molecule and electrode. The transmission decrease comes from the enhancement of electron scattering inside a molecule. We clarify the mechanism by which molecule-electrode coupling changes the magnitude of intramolecular scattering.

DOI: 10.1103/PhysRevB.81.085318 PACS number(s): 73.63.−b, 73.40.−c, 85.65.+h

I. INTRODUCTION

Since molecular junction systems are candidates for future nanoscale devices, their electron transport properties have attracted much attention and then much effort has been devoted to this field.[1] While, most of studies have concentrated on functionality of each junction system, the understanding over what determines transport properties is quite inadequate despite its importance for the fundamental science and practical applications.

It is well known that the transport properties strongly depend on the electronic state of a molecule,[2–7] since electrons travel between electrodes via molecular orbitals (MOs). Then, in many reports, the relation between the transport properties and the electronic state of an isolated molecule has been discussed. In the meanwhile, molecular electronic state is influenced by electrodes through the coupling between them, and thus strongly depends on the contact properties, such as atomic geometries, elements, and so on. While it has been reported that the difference in contact properties results in the difference in transport properties for many systems, the effect has not been systematically investigated so far. For the comprehensive understanding, it is indispensable to know the effect of a molecule-electrode contact on transport properties in detail.

In this paper, we theoretically revealed that molecule-electrode coupling plays a crucial role in electron transport properties. As the coupling becomes stronger, peaks of a transmission spectrum are lowered despite the increasing of the wave function hybridization between molecule and electrode. The transmission decrease comes from the enhancement of electron scattering inside a molecule. Then, we reveal the mechanism by which molecule-electrode coupling changes the magnitude of intramolecular scattering. To observe the effect, we investigate the transport properties of a junction system consisting of a biphenyl-dithiol (S-BP-S) molecule sandwiched between two Au electrodes [Fig. 1(a)], by using a nonequilibrium Green's function method based on the density functional theory (NEGF/DFT). Then, in order to clarify the role of molecule-electrode coupling, we performed model calculations and compared transmission-peak heights of the NEGF/DFT calculation with those of the model one.

II. CALCULATION DETAILS

The NEGF/DFT calculation are carried out by using the ASCOT code.[8] For a basis set, we employ the pseudo atomic orbitals, whose cutoff radius r_c and number of primitive orbitals are summarized in Table I.[9] We use the PW91 functional parameterized by Perdew and Wang for the exchange-correlation term[10] and Troullier–Martins type atomic pseudopotentials.[11] The energy cutoff for the real space mesh is 100 Ry.

The molecular structure is optimized using Gaussian 03 (PW91PL/LANL2DZ).[12] The optimization was performed for an isolated molecule whose S atoms were terminated with H atoms. Then those H atoms were removed and the molecule was sandwiched between Au electrodes. The molecule sits upright on the Au(111) surface with 3×3 periodicity and the S atom of each end is located at a hollow site.

III. RESULTS AND DISCUSSIONS

First, we investigate how molecule-electrode coupling affects the transmission spectrum. Here, to weaken the cou-

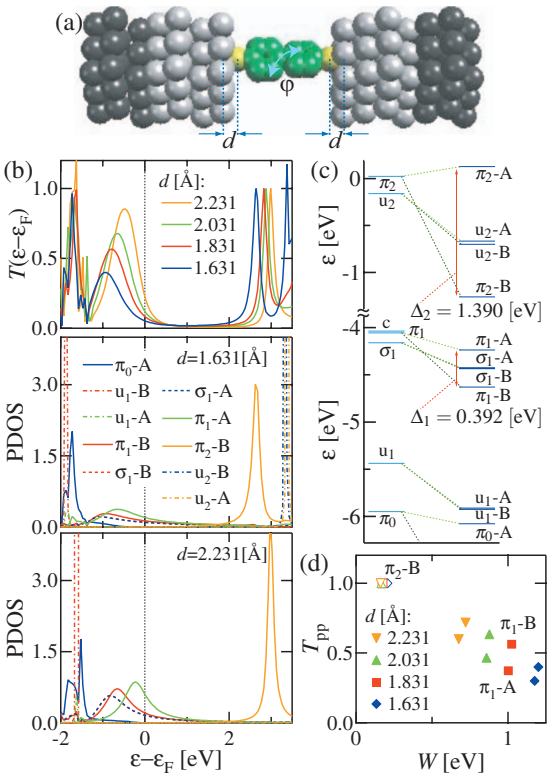

FIG. 1. (Color) (a) Atomic structure of the S-BP-S molecular junction system. (b) Distance (d) dependence of the transmission spectrum for the junction system (upper) and PDOS with respect to the MOs of an isolated S-BP-S molecule (middle and lower). (c) MO levels of an isolated S-BP-S molecule (right), accompanied with the MO levels of a half fragment [C_6H_4S] (left). With respect to the labels, such as π_1-B(A), see Ref. 13. Δ_2 (Δ_1) is the level splitting for the π_2 (π_1) orbital. (d) Transmission value T_{pp} at the PDOS-peak energy against the peak width W of PDOSs.

pling strength, the distance d between the S atom and the Au electrode surface in the junction system is elongated from the equilibrium one, 1.631 Å. This change in d also corresponds to the decrease of the wave function hybridization between molecule and electrode. The upper panel of Fig. 1(b) shows the d dependence of the transmission spectrum $T(\varepsilon-\varepsilon_F)$, where ε_F is the Fermi energy. $T(\varepsilon-\varepsilon_F)$ has a broad peak around $\varepsilon-\varepsilon_F \sim -1.0$ [eV] and a narrow one near $\varepsilon-\varepsilon_F \sim 2.5$ [eV]. While the former peak becomes higher with increasing d, the height of the latter remains 1 irrelevant to d. In other words, while electron scattering at peak energy becomes pronounced in the former, there is no electron scattering in the latter. The middle and lower panels of Fig. 1(b) show the projected density of states (PDOS) with respect to the S-BP-S MOs, whose names and energy levels are shown in the right side of Fig. 1(c).[13] The comparison between the PDOS and $T(\varepsilon-\varepsilon_F)$ shows that the transmission peaks around $\varepsilon-\varepsilon_F \sim -1.0$ [eV] and 2.5 [eV] arise from the π_1-B/A type MOs and the π_2-B type MO, respectively. The figure also shows that with increasing d the PDOS peaks become narrower and shift to higher energy.

TABLE I. Cutoff radius r_c of the pseudo atomic orbitals and number of the primitive orbitals for s, p, and d orbitals (n_s, n_p, and n_d) used in the calculations.

	r_c (a.u.)	n_s	n_p	n_d
Au	6.0	2	1	1
S	5.5	2	2	2
C	4.0	2	2	
H	4.0	2	2	

In order to clarify the role of molecule-electrode coupling in the electron transport, we investigate the relationship between the coupling and transmission-peak height. We here use half width of PDOS peak (W) to evaluate the coupling between each MO and the electrode ($V_{\text{MO-elec}}$), since PDOS-peak width indicates the strength of $V_{\text{MO-elec}}$.[14] The peak height is evaluated as the transmission value at the PDOS-peak energy,[15] and hereafter they are referred to as T_{pp}, where the subscript "pp" means "PDOS peak." In Fig. 1(d), the relationship between W ($V_{\text{MO-elec}}$) and T_{pp} is shown. From this figure, we find that the transmission-peak heights for the π_2-B type MO with weak $V_{\text{MO-elec}}$ (small W) have a value $T \sim 1$, while those for the π_1-B and π_1-A type MOs become lower with increasing $V_{\text{MO-elec}}$ (W). These results interestingly tell that *with increasing* $V_{\text{MO-elec}}$, *the electron scattering becomes stronger* despite the increasing of the wave function hybridization between molecule and electrode.

Now, we discuss where the electron scattering is enhanced. We first consider the molecule-electrode contact. In this regard, there is a noteworthy study.[16] For a junction system with one site between two electrodes, the transmission peak height is always 1, regardless of a molecule-electrode coupling. This indicates that the scattering around the molecule-electrode contact is irrelevant to the transmission peak height. Then, we speculate that the intra-molecular scattering changes depending on $V_{\text{MO-elec}}$. With respect to the intramolecular scattering, it has been reported that the transmission of an S-BP-S junction system strongly depends on the dihedral angle φ between the two phenyl rings.[3–6] The change in φ results in a change in the coupling between MOs of the two equivalent fragments, each consisting of a phenyl ring and a S atom. This result means that the intramolecular scattering depends on this coupling. Hereafter, we refer to the coupling as the intramolecule interaction V_{intra}. The strength of V_{intra} can be estimated from the level splitting Δ for each MO shown in the right side of Fig. 1(c).[17] We consider that this V_{intra} is relevant to the change in the transmission-peak height demonstrated above.

We investigate the mechanism by which V_{intra} and $V_{\text{MO-elec}}$ change the height of a transmission peak. However, it is difficult to extract only the roles of V_{intra} and $V_{\text{MO-elec}}$ from NEGF/DFT calculations. Then, in order to study their roles, we employ a model calculation in which two equivalent sites are sandwiched between two electrodes [Fig. 2(a)]. The two sites correspond to the two fragments of an S-BP-S molecule. The Hamiltonian of this model is expressed as,[5]

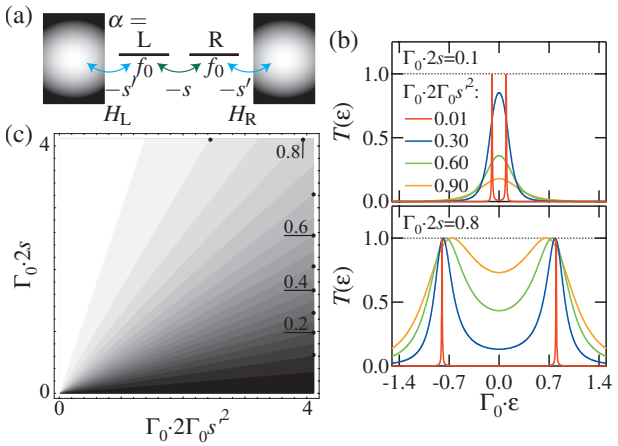

FIG. 2. (Color) (a) Two site model corresponding to the S-BP-S junction system. (b) $2\Gamma_0^2 s'^2$ dependence of the transmission spectrum $T(\varepsilon)$ for the model with $\Gamma_0 f=0$, and variable $2\Gamma_0 s$ ($2\Gamma_0 s=0.1$ and 0.8). (c) Contour map of the transmission value T_{pp}^m at the PDOS-peak energy $f \pm s$. A lighter (darker) area shows larger (smaller) transmission.

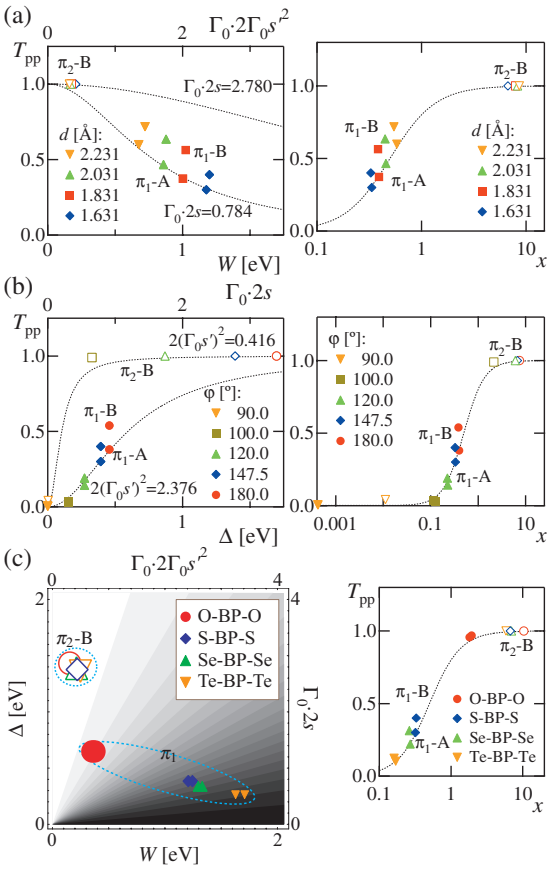

FIG. 3. (Color) Comparison of T_{pp} with T_{pp}^m: (a) d, (b) φ, and (c) end-group atom X dependencies (left) and the corresponding x expressions (right). The closed (open) symbols represent the $\pi_1(\pi_2)$ type MO. The dotted lines show the model calculation results. The values for $2\Gamma_0 s$ ($2\Gamma_0^2 s'^2$) shown in the left panels of (a) [(b)] are evaluated from Δ (W) obtained in the NEGF/DFT calculation. Size of symbols in the left panel of (c) indicates magnitude of T_{pp}.

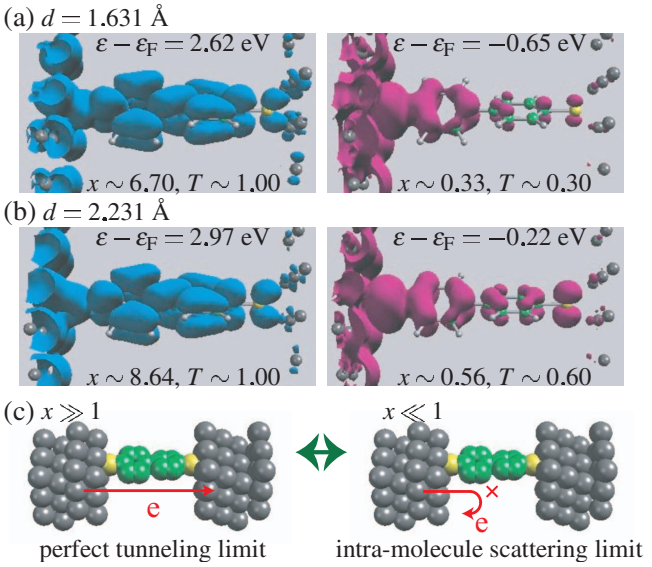

FIG. 4. (Color) (a) and (b) Charge density distribution $\rho^L(\mathbf{r},\varepsilon)$ for the electron starting in the left electrode for the junction system with d=1.631 Å (a) and 2.231 Å (b). For the plots, we use the same threshold values. (c) Schematic view of the electron scattering at PDOS peak energies in the limits of x.

$$\mathcal{H} = \sum_{\alpha=L,R} (f_0 d_\alpha^+ d_\alpha + H_\alpha) - (s' c_L^+ d_L + s d_L^+ d_R + s' d_R^+ c_R + \text{H.c.}), \tag{1}$$

where $H_{L(R)}$ are the Hamiltonians for the left(right) electrode, $c_{L(R)}^+$ and $d_{L(R)}^+$ are the creation operators for the electrode and the site on the left(right) sides, respectively, and $-s$ and $-s'$ are the transfer integrals and f_0 is an energy level for the two sites. The quantities $-s$ and $-s'$ correspond to V_{intra} and $V_{MO\text{-}elec}$, respectively. Eigenvalues for the sites $(f_0 \pm s)$ correspond to the MO levels of an isolated S-BP-S molecule. In this model, the level splitting Δ is $2s$. This type of model is often used for the analysis of electron transport.[18,19] We assume that the surface Green's function G_S is given as $G_S = \epsilon_0 - i\Gamma_0$ and therefore the DOS of the electrode surface is Γ_0/π. Here, for convenience, we also assume that Γ_0 and ϵ_0 are constant values with no energy dependence.[20] Then, the effective site energy is expressed as $f \equiv f_0 + s'^2 \epsilon_0$. In this calculation, we use $1/\Gamma_0$ as a unit of energy. The transmission spectrum $T(\varepsilon)$ is given as follows:

$$T(\varepsilon) = \frac{4s^2 \Gamma_0^2 s'^4}{[(\varepsilon - f + s)^2 + \Gamma_0^2 s'^4][(\varepsilon - f - s)^2 + \Gamma_0^2 s'^4]}. \tag{2}$$

We first discuss the calculated $T(\varepsilon)$ shown in Fig. 2(b). $T(\varepsilon)$ is formed as a superposition of two peaks located at $f \pm s$ and the half width W of them is calculated as $W = 2\Gamma_0 s'^2$. For small s', $T(\varepsilon)$ has two narrow peaks around the site energies $f \pm s$. Then, with increasing s', the peaks become wider and especially, if s is small, $T(\varepsilon)$ comes to have one-peak structure. We also obtain the same features as $T(\varepsilon)$ for the total DOS (not shown). The peak height of $T(\varepsilon)$ strongly depends on s and s', as shown in the figure. Figure 2(c) shows the transmission value T_{pp}^m (the index "m" means "model") at the

PDOS-peak energy $f \pm s$ as a function of Δ and W.[15] This T_{pp}^{m} is compared with the NEGF/DFT calculation and clearly shows the roles of V_{intra} and $V_{MO\text{-}elec}$, as the followings.

The comparison between the W-dependences of T_{pp} obtained from the NEGF/DFT calculation and T_{pp}^{m} from the model one is summarized in Fig. 3(a). Here, Γ_0/π is set to be $2/\pi$ [1/eV], according to the DOS of the Au surface at the Fermi energy, and therefore $\Gamma_0 \cdot 2s$ is evaluated to be 2.780 (0.784) for π_2 (π_1) type MO using the level splitting $\Delta_2=1.390$ [eV] ($\Delta_1=0.392$ [eV]) shown in Fig. 1(c). As seen in the left panel of the figure, T_{pp} are in good agreement with the model calculation.[21] This fact confirms that the two-site model is quite effective for modeling the S-BP-S molecular junction system. Namely, the transmission peak height of the system is well evaluated by the use of V_{intra} and $V_{MO\text{-}elec}$. From this figure, we find that the different W dependence between T_{pp} for the π_1 and π_2 type MOs comes from the difference in V_{intra}.

We here show the role of the two couplings for the transmission peak height. It is noteworthy that T_{pp}^{m} derived from Eq. (2) is expressed as

$$4x^2/(4x^2+1), \text{ using } x \equiv s/\Gamma_0 s'^2 = \Delta/W. \tag{3}$$

The left panel of Fig. 3(a) is then redrawn as the right one using x as a single independent variable. This figure clearly shows that all the calculated T_{pp} for the both MOs are in good agreement with the single curve of $T_{pp}^{m}(x)$. This means that peak heights can be evaluated using the unified form of $T_{pp}^{m}(x)$, irrelevant to MO types. Namely, the scaling of V_{intra} by $V_{MO\text{-}elec}$ is the very determinant for transmission peak height.

There are other aspects of the model calculation available aside from the d-dependence. First, the dependence on the dihedral angle φ between the phenyl rings is investigated. It has been reported that the transmission peak height increases with φ.[5] The left panel of Fig. 3(b) shows the φ dependence of T_{pp} expressed as the Δ dependence, accompanied with the corresponding Δ dependence obtained from the model calculation. This result shows that the difference between the Δ dependences of T_{pp} for the π_1 and π_2 type MOs arises from the difference in $V_{MO\text{-}elec}$. In the same way, the dependence of T_{pp} on end-group atom X is investigated. In Ref. 6, O, S, Se and Te were studied, as end-group atom X. As shown in the left panel of Fig. 3(c), the end-group atom has an influence on not only $V_{MO\text{-}elec}$ (W) but also V_{intra} (Δ). This figure also shows that the X dependences of T_{pp} are well evaluated by the use of these two coupling. These left panels are redrawn as the right ones using x, as well as Fig. 3(a). They clearly show that the x expression of T_{pp} is also available for the φ and X dependence. In addition, we have confirmed that it is applicable even for a change in electrode elements.[22]

In order to clarify where the intramolecular scattering is enhanced with decreasing x, we calculate the charge density distribution for the electron starting in the left electrode, i.e.,

$$\rho^{L}(\mathbf{r},\varepsilon) = \sum_{ij} \phi_i^*(\mathbf{r}) \rho_{ij}^{L}(\varepsilon) \phi_j(\mathbf{r}), \tag{4}$$

$$\rho_{ij}^{L}(\varepsilon) = -\frac{1}{\pi} \sum_{kl} G_{ik}^{r}(\varepsilon) \Im\{\Sigma_{kl}^{Lr}(\varepsilon)\} G_{lj}^{a}(\varepsilon), \tag{5}$$

where $G_{ik}^{r(a)}(\varepsilon)$, $\Sigma_{kl}^{Lr}(\varepsilon)$ and $\phi_i(\mathbf{r})$ are the Green's function, the self-energy of the left electrode and the pseudoatomic orbital, respectively. Figures 4(a) and 4(b) show the calculated $\rho^{L}(\mathbf{r},\varepsilon)$. The left panels show the case of large x, in which $T_{pp} \sim 1$ is obtained. It is found that the magnitude of $\rho^{L}(\mathbf{r},\varepsilon)$ at the left fragment of the S-BP-S molecule is almost the same as that at the right one. This shows that the electron scattering between the two fragments is negligible [perfect tunneling limit, the left panel of Fig. 4(c)]. In this case, the system can be regarded as a system consisting of a single site sandwiched between electrodes due to the strong V_{intra}.[16] On the other hand, in case of small x, as shown in the right panels, the magnitude of $\rho^{L}(\mathbf{r},\varepsilon)$ at the right fragment is quite smaller than that at the left one. This means that the electron scattering occurs between the two fragments [intramolecular scattering limit, the right panel of Fig. 4(c)]. It is noteworthy that the right panels also show the x dependence of the electron scattering, i.e., the magnitude at the right fragment in Fig. 4(a) is smaller than that in Fig. 4(b). We also confirmed that the charge density distribution for the electron starting in the right electrode has the same x dependence as $\rho^{L}(\mathbf{r},\varepsilon)$ [not shown]. In this way, it is clearly shown that the electron scattering between the two fragments is enhanced with decreasing x. It should be emphasized that even if V_{intra} stays constant, the change in $V_{MO\text{-}elec}$ causes the change in the intra-molecular scattering through the scaling of $x=\Delta/W$.

We discuss whether the change in intramolecular scattering due to molecule-electrode coupling occurs in other molecules. Here, as an example, we consider the junction system composed of a benzene dithiol (BDT) molecule and Au electrodes, whose transport properties have been well studied. As shown in Ref. 14, the on-top contact structure exhibits a higher T_{pp} for the σ type MO than the other contact structures. It is also shown that the on-top contact structure has a weaker $V_{MO\text{-}elec}$ than the others. However, the mechanism that determines peak heights had not been investigated at that time. Through the present analysis, it is considered that even in the BDT junction system the intramolecular scattering occurs, and it becomes more pronounced for larger $V_{MO\text{-}elec}$.[23] We consider that the enhancement of the intramolecular scattering due to $V_{MO\text{-}elec}$ is universal features for any molecular junction systems.

The enhancement of intramolecular scattering demonstrated in this paper has not been observed so far.[24] Here, it is noted that the recent developments in experiments can give high-resolution differential conductance with high reproducibility.[25] Such a differential conductance can be treated as an approximate transmission spectrum around the Fermi energy. We expect that transmission peak height and width would be estimated from it and the phenomena of the pronounced intramolecular scattering would be observed.

IV. CONCLUSIONS

In conclusion, thorough the theoretical investigation of the transport properties of a biphenyl-based molecular junc-

tion system, we revealed the relationship between $V_{\text{MO-elec}}$ and electron scattering. It is found that the transmission peak height T_{pp} decreases with increasing $V_{\text{MO-elec}}$ through the enhancement of the intramolecular scattering. The magnitude of T_{pp} is determined using the ratio $x=\Delta/W$, which is the scaling of V_{intra} by $V_{\text{MO-elec}}$. We expect that the enhancement of the intramolecular scattering due to $V_{\text{MO-elec}}$ could be observed for other molecular junction systems.

ACKNOWLEDGMENTS

This study was partially supported by the RISS project of MEXT of the Japanese Government.

[1] A. Aviram and M. A. Ratner, Chem. Phys. Lett. **29**, 277 (1974); C. Joachim, J. K. Gimzewski, and A. Aviram, Nature (London) **408**, 541 (2000).

[2] For reviews, A. Nitzan and M. A. Ratner, Science **300**, 1384 (2003); M. Koentopp, C. Chang, K. Burke, and R. Car, J. Phys.: Condens. Matter **20**, 083203 (2008) and references therein.

[3] M. P. Samanta, W. Tian, S. Datta, J. I. Henderson, and C. P. Kubiak, Phys. Rev. B **53**, R7626 (1996).

[4] F. Pauly, J. K. Viljas, J. C. Cuevas, and G. Schon, Phys. Rev. B **77**, 155312 (2008).

[5] H. Kondo, J. Nara, H. Kino, and T. Ohno, J. Chem. Phys. **128**, 064701 (2008).

[6] H. Kondo, J. Nara, H. Kino, and T. Ohno, Jpn. J. Appl. Phys. **47**, 4792 (2008).

[7] J. K. Tomfohr and O. F. Sankey, Phys. Status Solidi **233**, 59 (2002); J. Chem. Phys. **120**, 1542 (2004).

[8] The ASCOT code is developed within the RISS project supported by MEXT of the Japanese government. For the detail of this code, see Ref. 6.

[9] T. Ozaki, Phys. Rev. B **67**, 155108 (2003).

[10] J. P. Perdew and Y. Wang, Phys. Rev. B **45**, 13244 (1992).

[11] N. Troullier and J. L. Martins, Phys. Rev. B **43**, 1993 (1991); L. Kleinman and D. M. Bylander, Phys. Rev. Lett. **48**, 1425 (1982).

[12] M. J. Frisch *et al.*, Gaussian, Inc., Wallingford CT, 2004.

[13] The name of each MO, such as π_1-$B(A)$, indicates the name of a constituent MO of a half fragment (C_6H_4S) of an S-BP-S molecule and the bonding (B) or antibonding (A) state. The details of this naming system are given in Refs. 5 and 6.

[14] H. Kondo, H. Kino, J. Nara, T. Ozaki, and T. Ohno, Phys. Rev. B **73**, 235323 (2006).

[15] T_{pp} is the transmission peak value, when the peak has a contribution from only one MO. However, when the transmission peak arises from several MOs, the contribution from an individual MO cannot be definitely determined.

[16] H. Kondo, H. Kino, and T. Ohno, Phys. Rev. B **71**, 115413 (2005).

[17] This arises from the fact that each MO of an S-BP-S molecule is composed of two same types of fragment MOs and mixing of different types of fragment MOs is quite small. For details, see Refs. 5 and 6.

[18] J. Heurich, F. Pauly, J. C. Cuevas, W. Wenzel, and G. Schön, arXiv:cond-mat/0211635 (unpublished); J. C. Cuevas, J. Heurich, F. Pauly, W. Wenzel, and G. Schön, Nanotechnology **14**, R29 (2003); P. Delaney, M. Nolan, and J. C. Greer, J. Chem. Phys. **122**, 044710 (2005).

[19] K. S. Thygesen, Phys. Rev. Lett. **100**, 166804 (2008); P. Myöhänen, A. Stan, G. Stefanucci, and R. van Leeuwen, Europhys. Lett. **84**, 67001 (2008).

[20] This assumption does not have any qualitative influence on the discussion.

[21] T_{pp} for the π_1-B type MO is evaluated to be slightly larger than T_{pp}^{m}. This is because the π_0-A type MO partially contributes to T_{pp} evaluated for the π_1-B type MO.[15]

[22] H. Kondo, J. Nara, H. Kino, and T. Ohno, J. Phys.: Condens. Matter **21**, 064220 (2009).

[23] H. Kondo, J. Nara and T. Ohno (unpublished).

[24] For experimental reviews, R. L. McCreery, Chem. Mater. **16**, 4477 (2004); D. K. James and J. M. Tour, *ibid.* **16**, 4423 (2004) and references therein.

[25] For example, J. Reichert, H. B. Weber, M. Mayor, and H. v. Löhneysen, Appl. Phys. Lett. **82**, 4137 (2003).